Self-assembled epitaxial magnetic lateral structures on Ru: Controlling the shape and placement

Ruihua Cheng,[1] J. Pearson, H. F. Ding,[1] Vitali Metlushko,[2] S. D. Bader,[1] F. Y. Fradin,[1] and Dongqi Li[1,*]
[1]*Materials Science Division, Argonne National Laboratory, 9700 S. Cass Avenue, Argonne, Illinois 60439*
[2]*Department of Electrical & Computer Engineering, University of Illinois, Chicago, Illinois 60607, USA*
(Received 6 October 2003; revised manuscript received 8 December 2003; published 19 May 2004)

We explore lithographic patterning and substrate orientation of single-crystal Ru substrates as the means to control shape, alignment, and magnetic anisotropy of epitaxial Co and Fe islands. The Co dots and stripes were grown at 350 °C via molecular-beam epitaxy and characterized *ex situ* with atomic force microscopy, magnetic force microscopy, and the magneto-optic Kerr effect. For Co deposited onto a Ru(0001) pre-etched with deep 6×6 μm squares, Co islands decorate the edges of the patterns and exhibit in-plane magnetic domains with easy axis along the edges. Shallow patterns, however, do not result in preferential positioning of the dots. When the etched shallow lines are along the close-packed $[10\bar{1}0]$ direction, the islands tend to elongate along the induced steps, which introduces a magnetic easy axis along the line direction. In contrast to the quasihexagonal dots of Co on Ru(0001), Fe deposited on the twofold Ru$(10\bar{1}1)$ forms elongated islands of ~100 nm long and 20 nm wide.

DOI: 10.1103/PhysRevB.69.184409 PACS number(s): 75.75.+a, 75.30.Gw, 68.37.Ps

I. INTRODUCTION

Magnetic nanostructures are of great interests in recent years due to their technical applications as well as their rich fundamental physics.[1] Self-assembly is becoming a powerful approach to fabricate arrays of nanostructures quickly and at low cost.[1–5] These nanostructures are not constrained by the physical lithographic length scale limits, and tend to be thermodynamically stable. A fundamental challenge of self-assembly is the control in shape and placement of these structures. Lithography-guided self-assembly growth appears promising to realize the best aspects of both approaches,[6] which may allow the positioning of small self-assembled nanostructures with larger length scale lithography patterns. For semiconducting self-assembled quantum dots, regular dot arrays were indeed grown successfully onto lithographically patterned substrates.[7–10] No comparable work of growth on lithographically patterned substrate, however, has been reported for magnetic materials.

Recently we reported that quasihexagonal Co magnetic dots grew on flat Ru(0001) substrates[11] and that Co dot chains grew on grooved Ru(0001) substrates.[6,12] Both the lateral size of these Co dots and the interdot distance can be controlled by substrate temperature and coverage. This Stranski-Krastanow (SK) growth mode, which consists of a thin wetting layer followed by three-dimensional island growth,[13–16] has been shown to be an effective approach to make magnetic dot arrays.[6,11,12] The Co dots form single domains with an in-plane magnetic easy axis, and are coupled along the chains via magnetostatic interactions.[12,17] Although Ref. 6 demonstrated the promise of manipulating dot alignment with substrate modification, the grooves were made with polishing scratches and step bunching during annealing instead of via well-defined lithography. In this paper, we control lateral magnetic nanostructures via substrates by means of two different approaches. First, we explored lithographic patterning of the substrate to guide SK mode self-assembly by depositing Co onto a patterned Ru(0001) substrate. Secondly, we choose Ru$(10\bar{1}1)$ which has different (twofold) symmetry—and deposit Fe on it. We demonstrate that the steep edges etched via lithography can indeed trap Co along the edges as seen on our square patterns. For edges that are gradual and continuous, as in our line patterns, however, the positions of the dots are more random. When the lines, and therefore the induced steps are along the close-packed $[10\bar{1}0]$ direction, we observe modified shapes of elongated islands and nanowires. The increased step density alters the atom diffusion on the surface, especially when the lithographic lines are along a high-symmetry direction of Ru(0001) substrate. Such an asymmetry in island shape is also observed in Fe growth onto flat Ru$(10\bar{1}1)$ substrate, where Fe forms rectangular islands. Our results indicate that lithographically guided self-assembly is a versatile approach for organizing complex nanomaterials.

II. EXPERIMENTAL APPROACH

Two single-crystal substrates, i.e., Ru(0001) and Ru$(10\bar{1}1)$, were used as substrates for the epitaxial growth. While Ru$(10\bar{1}1)$ was kept flat, e-beam lithography was utilized to create three types of patterns on the same Ru(0001) substrate. For deep patterns with edges far apart, 6×6 μm^2 square arrays with 10.5 μ m repeat period were etched. For shallow patterns, 750 nm-wide lines with 1.5 μ m periods, either perpendicular or parallel to $[10\bar{1}0]$, were produced. The sample fabrication process began with the spin coating of a Ru(0001) crystal with the positive-type e-beam resist. The pattern was written with e-beam lithography and developed. The resist mask defined the pattern that was being etched. Argon milling was performed in a veeco ion milling system with the Ru crystal attached to a rotating water-cooled stage. The system used Ar ions from a broad-beam source to ion mill material without the use of any chemistry. The rotating cold stage assured uniform etching of the Ru crystal while maintaining surface temperatures below 100 °C. After removing the resist layer with O_2 plasma etch-

ing, the square patterns and line patterns were ~110 and ~20 nm in depth, respectively, while later high temperature annealing in vacuum reduced them to ~100 nm and ~5 nm. The depth difference between the two types of patterns is partly due to the feature size difference, which can strongly affect etching rate,[18] and partly due to Ru atom diffusion during high-temperature flashings, which tends to smooth out the surface. The bare, patterned Ru(0001) or flat Ru(10$\bar{1}$1) substrates were transferred into an ultrahigh-vacuum (UHV) chamber with a base pressure of $<1.0\times10^{-10}$ Torr for *in situ* cleaning and growth. The crystals were cleaned *in situ* with multiple cycles of oxygen annealing at 1200–1300 K with O_2 pressure of 2×10^{-8} Torr, followed by flash annealing at 1500–1600 K.[6,11] The repeated flash annealing of the patterned substrate tends to smooth out the surface as mentioned. The sloped edges for the squares laterally extend ~1 μm, forming highly stepped regions in contrast to the flat Ru(0001) regions at the top and bottom. The four edges of the square are not exactly the same after the annealing. Since the line patterns have spacing of 750 nm, this region becomes completely stepped with alternating slopes after annealing, with no remaining flat region.

Co was evaporated onto the patterned Ru(0001) substrate at a deposition rate of 0.25 Å/min with a wedge-shape thickness gradient from one end of the substrate to the other with nominal Co thickness of 0–0.9 nm at an elevated substrate temperature of 350 °C. This temperature is chosen because it is known to produce three-dimensional Co islands with smooth edges and tops,[6,11] while lower temperatures result in continuous films.[19] As a comparison to growth on the sixfold symmetric Ru(000$\bar{1}$) substrate, 0.1 nm of Fe was deposited onto the Ru(10$\bar{1}$1) substrate at a slow growth rate of 0.07 Å/min with the substrate temperature at ~350 °C. It has twofold symmetry and therefore likely asymmetric adatom diffusion. During the Co and Fe deposition, the vacuum pressure in the chamber was 6×10^{-10} Torr. Both the substrates and the Co and Fe are free of contamination of oxygen and carbon as the Auger electron spectroscopy measurements indicate within its detection limit of a few percent. The low-energy electron-diffraction (LEED) patterns of the substrates and Co samples show sharp spots with no reconstruction and negligible background, indicating a high degree of crystalline ordering on the surface. In order to prevent oxidation during *ex situ* measurements, the samples were then covered with a thin layer of Au (<1 nm) before they were taken out of the UHV chamber. The morphology and magnetic domain structures were characterized *ex situ* using atomic force microscopy (AFM) and magnetic force microscopy (MFM). The magnetic anisotropy of the patterned sample was also studied *ex situ* with the longitudinal magneto-optical Kerr effect (MOKE) at room temperature by applying a magnetic field in plane along various azimuthal directions.

III. RESULTS AND DISCUSSION

A. Co on lithographically patterned Ru(0001)

Figure 1 shows (a) the AFM and (b) MFM images of Co dots at a nominal coverage of 0.6 nm on the patterned

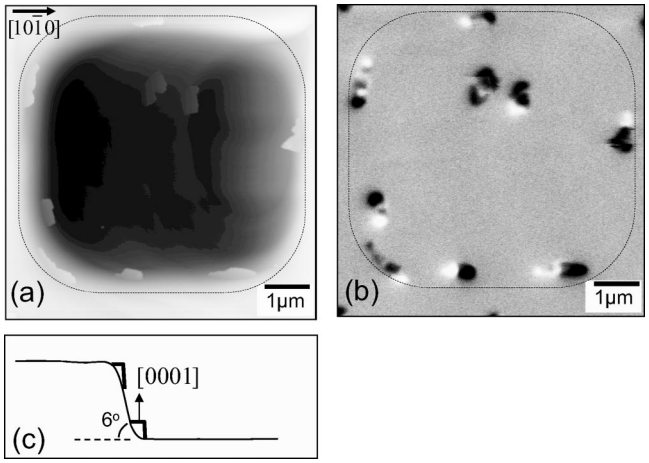

FIG. 1. (a) AFM and (b) corresponding MFM images of Co islands grown on the lithographically patterned Ru (0001) substrate with $6\times6\ \mu m^2$ squares. The scan size for both images is $7\times7\ \mu m^2$. The Co islands mainly grow along the edges of the square, and exhibit in-plane easy axis along the edges. (c) Schematic line profile across a deep edge showing the locations of the dots at the top or bottom of the edges.

Ru(0001) substrate around the 6 μ m squares of ~100 nm deep. The dotted lines mark the top edges of the square with rounded corners. It is clear that most of the Co islands locate at either the top (close to the dotted lines in Fig. 1) or the bottom of the edges (slightly away from the lines, inside the dotted squares in Fig. 1), while only a few stay at the relatively flat bottom near the middle of the square, where some residual steps exist. Figure 1(c) is a schematic drawing of the side-view profile of an edge, where the Co dots sit at its top and/or bottom. The top surfaces of the Co are always parallel to the (0001) basal plane. This is consistent with our previous results on grooved substrates, where the quasi hexagonal dots line up along the top and/or bottom of the edges.[6] Even when the lithographic edge curves at the corners, the Co islands still align along the edges, as illustrated at the lower left corner of Fig. 1(a). We postulate that such placement along the edges is a result of different surface diffusion rates of Co on the flat surfaces at the bottom and top, and the stepped surfaces on the sloped edges. When the Co atoms diffuse from the fast-diffusion regions of flat Ru(0001) to slow-diffusion regions of stepped Ru(0001) on the etched slopes, they nucleate and form islands. To our knowledge, there is no measurement on the diffusion rate of Co on stepped Ru, though it is common for the adatoms to experience a barrier at the step edges, which results in slower diffusion.[20] Alternatively, the dots may also nucleate because of the changes in strain as the substrate surface curvature changes. Our results, however, do not favor such an explanation, since the dots normally locate at a side, instead of right on the points with the largest curvature change.[6] The islands in Fig. 1(a) are elongated with lateral sizes of ~250 nm wide, ~15 nm high, and ~700 nm–1 μm long, many appearing as a group of connected dots. The shapes of the dots are less regular compared with the previous quasi-hexagonal dots on the flat and grooved Ru(0001),[6,11] possibly because the Ru surface is slightly degraded by ion bom-

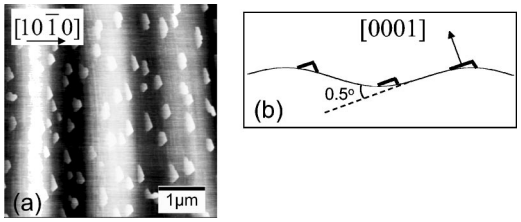

FIG. 2. (a) AFM image ($5\times5\ \mu m^2$) of Co grown on the patterned Ru (000$\bar{1}$) substrate with shallow 750 nm wide lines perpendicular to [10$\bar{1}$0] direction. (b) Schematic line profile across the shallow lithographic lines. The dots are not confined enough, as discussed in the text.

bardment or impurities during the lithographic processing, even after cycles of flash annealing.

Figure 1(b) is the corresponding MFM image on the same square that shows alternating bright and dark contrast along the edges. Since our MFM measurements are sensitive to the magnetic-field gradient, each pair of dark and bright contrast indicates the ends of an in-plane magnetic domain. This indicates that the magnetic domains are in plane. The magnetic easy axis is always along the edges, even when they curve around the corners as defined by the lithographic process. This provides additional control over magnetic properties when guiding self-assembly growth with lithography. Several of the apparent stripes exhibit multiple domains, suggesting that they consist of connecting Co dots, each having a single domain and separated by magnetic domain walls. It is known that the magnetostatic interaction along a magnetic dot chain, each dot having a single domain, can introduce an additional magnetic uniaxial anisotropy with easy axis along the chain direction.[17] This could explain the easy axis along the lithographic edges. We do not, however, rule out the influence of atomic step edges to the magnetocrystalline anisotropy of the Co, which could also induce additional anisotropy either along or perpendicular to the steps.[21–23] As expected, no uniaxial magnetic anisotropy was observed with MOKE at the square-patterned regions, since the laser spot averages over all the edges along the two perpendicular directions to make the over-all anisotropy fourfold instead of twofold as seen in MFM. It should be noted that the unpaired contrast, such as the dark feature at the bottom plane of the square [see Fig. 1(b)] is the result of tip-sample magnetic interactions that flip the domains during the scans. Such interactions are often seen when the magnetic anisotropy, and therefore the barrier for magnetic reversal is low.

While the steep edges are selectively decorated, shallow patterns with gradual slope change do not appear to align the dots as well. The Co growth on line-patterned Ru(0001) with the edges perpendicular to [10$\bar{1}$0] is illustrated in Fig. 2 for Co nominal thickness of $\sim$0.5 nm. After the substrate cleaning process, the 750 nm wide line patterns are significantly smeared out, though still visible from the contrast modulation in Fig. 2(a). The depths of the patterns are reduced to $\sim$5 nm with gradual slopes, instead of having well-defined edges as in Fig. 1. The dots distribute randomly on the surface, though the top and bottom sites are still slightly preferred. Figure 2(b) shows a schematic drawing of the side-view profile of the etched substrate and the dots on it, indicating the continuous variation of the surface slope and less selectivity of the dot placement. Note that the features on this surface are much more shallow. And the angle of the sloped edges is much smaller [0.5°, vs 6° as in Fig. 1(c)]. In other words, the whole surface became slightly stepped with no flat regions. This dictates that the diffusion rate over the whole surface changes only slowly. And there is no abrupt slope change to introduce additional strain. Therefore, the islands distribute all over the surface instead of along far-spaced edges, where the flat and stepped surfaces meet.

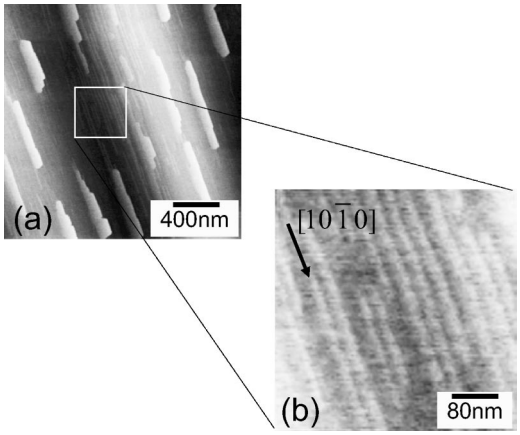

FIG. 3. AFM images of Co grown on the Ru (0001) substrate with shallow 750 nm wide patterned lines parallel to the [10$\bar{1}$0] direction. The images were taken at the same region with different magnifications with scan sizes of (a) $2\times2\ \mu m^2$. and (b) $400\times400\ nm^2$.

When the etched lines are along the [10$\bar{1}$0] direction, although the positions of the Co islands are still random, the shapes of the islands change to elongated stripes of $\sim$100 nm wide, 500 nm–1 μm long, and 3 nm high, and finer nanowires with width of $\sim$20 nm, as seen both in Fig. 3(a) and more clearly in Fig. 3(b) in the zoom-in images. The long stripes are produced when the lithographic lines are along a high-symmetry direction, Ru [10$\bar{1}$0] or the equivalent direction, while dots form when the lines are perpendicular to it or along an arbitrary direction. The high step density along [10$\bar{1}$0] or equivalent directions breaks the sixfold symmetry of Ru(0001) and introduces significant asymmetry in adatom diffusion and mass transport. This affects the island shape significantly.[24] Furthermore, when the steps are along the high-symmetry direction, the defects introduced in the lithographic process appear to be relaxed or eliminated to a large extent, and the wires grow into regular shapes with smooth edges.

Figure 4 shows the in-plane magnetic hysteresis loops of Co grown on the line patterns roughly along [10$\bar{1}$0] obtained via longitudinal MOKE measurements at room temperature. The solid line shows the magnetic hysteresis loop with magnetic field applied along the etched lines, and therefore mostly along the Co wires, while the dotted line is for the field perpendicular to the patterned lines. The full remanence of the solid line data indicates that the magnetic easy axis is along the wire direction. This is consistent with the

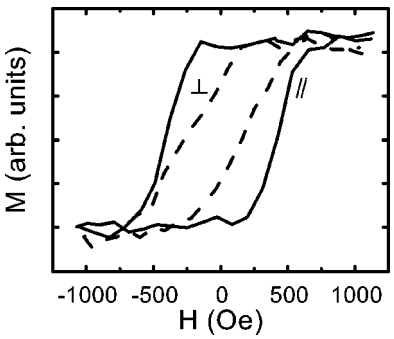

FIG. 4. In-plane hysteresis loops of Co nanowires grown on line patterned Ru(0001) substrate measured by means of longitudinal MOKE at room temperature. The solid line shows the result with the magnetic field along the axis of the nanowires. The dashed line shows the result with magnetic field perpendicular to the axis of the nanowires.

shape anisotropy along the long axis of the wires, though we do not rule out the contribution of step-induced magnetocrystalline anisotropy. The magnetic properties obtained from MOKE is the average of the long wires, the shorter stripes, as well as some dots in the line-patterned region due to the finite size of the laser beam of $\sim 1 \times 1$ mm. This explains why there is still finite remanent magnetization perpendicular to the etched lines.

At different nominal Co thickness, both the density and size of the dots/wires increase in a similar fashion as on flat Ru(0001).[11,19] Their positioning and shape variations on the lithographically etched substrate, however, are *not* significantly affected by nominal thickness.

B. Fe on flat Ru($10\bar{1}1$)

To investigate how the symmetry of a substrate affects island shape, we chose a twofold Ru($10\bar{1}1$) substrate for comparison with the Ru($000\bar{1}$). Figure 5(a) shows the LEED pattern of the clean Ru($10\bar{1}1$), which clearly exhibits twofold symmetry. Figure 5(b) exhibits the corresponding real-space lattice that is consistent with the LEED pattern, confirming that the surface is indeed Ru($10\bar{1}1$). (The surface orientation was also independently verified *ex situ* with x-ray diffraction.) Figure 6 shows the AFM images of submonolayer Fe on Ru($10\bar{1}1$). The high-symmetry direction is marked in Fig. 6(a). The atomic steps of the substrate are $\sim 45°$ away from the [0110] direction. The average size of the terraces is ~ 130 nm while some terraces are wider. Fe forms elongated patches that are one atomic layer high, ~ 100 nm long, and 20 nm wide. They are quite different from the quasihexagonal Co dots grown on flat Ru(0001) (see Fig. 6 (c)). The long axis of these patches is along [0110], the close-packed chain direction. This is similar to the growth of Fe on Mo(110), where rectangular islands with long axes along the close packed Mo[001] direction were observed.[25] The island shape has been attributed to the variation of the step free energy with angle at equilibrium and asymmetric diffusion away from equilibrium,[26–29] both of which are affected by the asymmetric bonding of adatoms.[30–32] The long edges are normally along the fast diffusion directions, though examples of elongated islands and atomic chains perpendicular to the fast diffusion direction have also been observed previously.[31,33] Nevertheless, our results offer another example where the island shape is determined by the symmetry of the substrate.

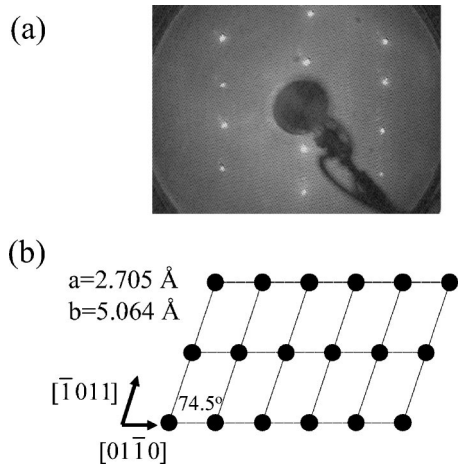

FIG. 5. (a) LEED pattern of flat Ru($10\bar{1}1$) substrate [electron energy at 113.6 eV]. (b) Real-space lattice structure of the Ru($10\bar{1}1$) surface.

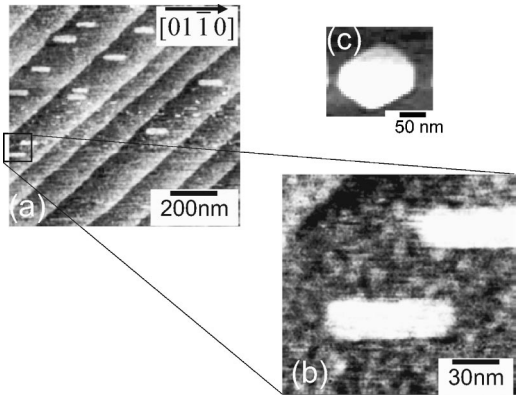

FIG. 6. AFM images of Fe nanodots on flat Ru($10\bar{1}1$) substrate with scan sizes of (a) $1 \times 1\ \mu m^2$ and (b) $150 \times 150\ nm^2$. (c) For comparison, quasihexagonal Co dots on flat Ru(0001).

At room temperature, no ferromagnetic signal was detected from either longitudinal or polar MOKE in the magnetic-field range between ± 3 KOe at room temperature, possibly because the patches are too thin and have a Curie temperature below room temperature.

IV. CONCLUSION

We have explored the control of shape, alignment, and magnetic anisotropy of magnetic lateral structures with either lithographically guided self-assembly or growth on substrates of different symmetry. The Co islands aligned along the deep edges of the lithographic patterns on Ru(0001), at the top or bottom where the steep slope meets the flat (0001) surface. Gradual slope changes introduced by shallow,

closely spacedline patterns, however, do not result in site selectivity of the island growth. The induced magnetic easy axis of Co on Ru is always along the lithographic edges, regardless of the depth of the patterns. The induced steps along a close-packed direction can change the shape of the islands to elongated stripes and fine wires. The shape of the islands can also be controlled by the choice of substrate symmetry as seen for Fe on Ru(1011). These results demonstrate that it is indeed possible to control the shape, alignment, and magneticproperties of self-assembled, MBE grown magnetic nanostructures.

ACKNOWLEDGMENTS

We would like to thank Chengtao Yu and Jon M. Hiller for technical assistance. This work was supported by the U.S. DOE BES-Materials Sciences under Contract No. W-31-109-ENG-38, and the U.S. NSF, grants Nos. ECS-0202780 and DMR-0210519 (VM).

*Author to whom correspondence should be addressed. Email address: dongqi@anl.gov

[1] F.J. Himpsel, J.E. Ortega, G.J. Mankey, and R.F. Willis, Adv. Phys. **47**, 511 (1998).
[2] F. Komori, S. Ohno, and K. Nakatsuji, J. Phys.: Condens. Matter **14**, 8177 (2002).
[3] P. Politi, G. Grenet, A. Amarty, A. Ponchet, and J. Villain, Phys. Rep. **324**, 271 (2000).
[4] Dongqi Li, Verena Diercks, J. Pearson, J.S. Jiang, and S.D. Bader, J. Appl. Phys. **85**, 5285 (1999).
[5] K. Asakawa, T. Hiraoka, H. Hieda, M. Sakurai, Y. Kamata, and K. Naito, J. Photopolym. Sci. Technol. **15**, 465 (2002).
[6] Chengtao Yu, Dongqi Li, J. Pearson, and S.D. Bader, Appl. Phys. Lett. **79**, 3848 (2002).
[7] G. Jin, J.L. Lie, S.G. Thomas, Y.H. Luo, K.L. Wang, and B.Y. Nguyen, Appl. Phys. Lett. **75**, 2752 (1999).
[8] O.G. Schmidt, N.Y. Jin-Phyllipp, C. Lange, U. Denker, K. Eberl, R. Schreiner, H. Grabeldinger, and H. Schwerzer, Appl. Phys. Lett. **77**, 4139 (2000).
[9] P.M. Petroff, A. Lorke, and A. Imamoglu, Phys. Today **54** (5), 46 (2001).
[10] B. Yang, F. Liu, A.R. Woll, and M.G. Lagally (unpublished); M.G. Lagally and P. Rugheimer, Jpn. J. Appl. Phys., Part 1 **41**, 4863 (2002).
[11] Chengtao Yu, Dongqi Li, J. Pearson, and S.D. Bader, Appl. Phys. Lett. **78**, 1228 (2001).
[12] Dongqi Li, Chengtao Yu, J. Pearson, and S.D. Bader, Phys. Rev. B **66**, 020404(R) (2002).
[13] D. Bimberg, M. Grundmann, and N. Ledentsov, *Quantum Dot Heterostructures* (Wiley, New York, 1999).
[14] I. Daruka and A.L. Barabasi, Phys. Rev. Lett. **79**, 3708 (1997).
[15] V. Shchukin and D. Bimberg, Rev. Mod. Phys. **71**, 1125 (1999).
[16] G. Springholz, M. Pinczolits, P. Mayer, V. Holy, G. Bauer, H. Kang, and L. Salamanca-Riba, Phys. Rev. Lett. **84**, 4669 (2000).
[17] Chengtao Yu, J. Pearson, and Dongqi Li, J. Appl. Phys. **91**, 6955 (2002).
[18] S.A. Campbell, *The Science and Engineering of Microelectronic Fabrication* (Oxford University Press, New York, 1996).
[19] H.F. Ding, A.K. Schmid, Dongqi Li, K.Y. Guslienko, and S.D. Bader (unpublished).
[20] G.L. Kellogg, Surf. Sci. Rep. **21**, 1 (1994).
[21] H.J. Choi, R.K. Kawakami, E.J. Escorcia-Aparicio, Z.Q. Qiu, J. Pearson, J.S. Jiang, Dongqi Li, and S.D. Bader, Phys. Rev. Lett. **82**, 1947 (1999).
[22] A. Berger, U. Linke, and H.P. Oepen, Phys. Rev. Lett. **68**, 839 (1999).
[23] H.J. Choi, R.K. Kawakami, E.J. Escorcia-Aparicio, Z.Q. Qiu, J. Pearson, J.S. Jiang, Dongqi Li, and S.D. Bader, Phys. Rev. Lett. **82**, 1947 (1999).
[24] C. Günther, S. Günther, E. Kopatzki, R.Q. Hwang, J. Schröder, J. Vrijmoeth, and R.J. Behm, Ber. Bunsenges. Phys. Chem. **97**, 522 (1993).
[25] P.O. Jubert, O. Fruchart, and C. Meyer, Phys. Rev. B **64**, 115419 (2001).
[26] D.C. Schlößer, L.K. Verheij, G. Rosenfeld, and G. Comsa, Phys. Rev. Lett. **82**, 3843 (1999).
[27] Y. Li, M.C. Bartelt, J.W. Evans, N. Waelchli, E. Kampshoff, and K. Kern, Phys. Rev. B **56**, 12 539 (1997).
[28] K. Morgenstern, E. Lagsgaard, I. Stensgaard, and F. Besenbacher, Phys. Rev. Lett. **83**, 1613 (1999).
[29] M.C. Bartelt, A.K. Schmid, J.W. Evans, and R.Q. Hwang, Phys. Rev. Lett. **81**, 1901 (1999).
[30] I.N. Yakovkin, G.A. Katrich, A.T. Loburets, Y.S. Vedula, and A.G. Naumovets, Prog. Surf. Sci. **59**, 355 (1998).
[31] Q.M. Braun and V.K. Medvedev, Sov. Phys. Usp. **32**, 328 (1989).
[32] Y.B. Losovyj, I.N. Yakovkin, S.D. Barrett, T. Komesu, and P.A. Dowben, Surf. Sci. **520**, 43 (2002).
[33] Y.-W. Mo, J. Kleiner, M.B. Webb, and M.G. Lagally, Phys. Rev. Lett. **66**, 1998 (1991).